Semi-solid slurry preparation, rheo-die casting and rheo-squeeze casting of an AZ91–2Ca–1.5Ce ignition-proof magnesium alloy by gas-bubbling process

Jimei Mao, Wencai Liu,[a)] and Guohua Wu[b)]
National Engineering Research Center of Light Alloy Net Forming and State Key Laboratory of Metal Matrix Composites, School of Materials Science and Engineering, Shanghai Jiao Tong University, Shanghai 200240, China

Jianfeng Fan
Key Laboratory of Interface Science and Engineering in Advanced Materials, Ministry of Education, Taiyuan University of Technology, Taiyuan 030024, China

Daqiang Cheng, Guangling Wei, Liang Zhang, Wenjiang Ding, and Chaoying Xie
National Engineering Research Center of Light Alloy Net Forming and State Key Laboratory of Metal Matrix Composites, School of Materials Science and Engineering, Shanghai Jiao Tong University, Shanghai 200240, China

In present study, the semi-solid slurry of the AZ91–2Ca–1.5Ce alloy was firstly prepared by gas-bubbling processing and then was formed by die casting and squeeze casting, respectively. The influence of processing parameters on microstructure and mechanical properties of the alloy was investigated. The results show that increase of gas-flow rate and appropriate pouring temperature can improve the quality of the semi-solid slurry and change the morphology of primary α-Mg particles to rosette-like shape or roundness. Meanwhile, the addition of calcium and cerium refines the as-cast microstructure and dramatically improves the tensile properties, also the strengthening phase Al$_4$Ce exists around the grain boundary. The peak ultimate tensile strength (UTS), yield strength, and elongation of rheo-die casting AZ91–2Ca–1.5Ce alloy are 202 MPa, 154 MPa, and 2.3%, respectively. Especially, compared with conventional liquid die-casting, the UTS and elongation of rheo-die casting AZ91–2Ca–1.5Ce alloy were improved by 8% and 64%, respectively. Meanwhile, the rheo-die casting alloy also showed higher mechanical properties than rheo-squeeze casting alloy, since the higher speed that die casting provided could induce more compact microstructure and remain the semi-solid characteristic better.

I. INTRODUCTION

As environment pollution and energy consumption became the world's focuses, much funds and research have been given to light materials for industrial application.[1,2] Because of their high strength, low density, outstanding castability, and advanced damping characteristics, magnesium alloys are becoming a potential material to be applied in the motorcars, aerospace, and electrical equipment.[3,4] The high-pressure die casts are most commonly used in automotive casting components.[5,6] Among the wide variety of Mg alloys, the Mg–Al–An (AZ) series alloys are the most widely available and used in the manufacturing industry,[7] in which the AZ91 alloy is a much more widely-used die casting magnesium alloy for automotive parts including crankcase, cam covers, oil pan, clutch housing, etc.[8–10] However, the performance of AZ91 alloy needs to be further improved to meet the requirements of more fields.[11] During the decade, an amount of researches have adopted the way of adding other alloy elements such as rare-earth, Si, Sr, and Ca to the AZ91 alloy to further improve the performance of the base alloy.[12–15] Meanwhile, alloying with Ce in some type of Mg alloy is a powerful method in refining the microstructures and improving the mechanical properties.[16] As has been reported, Ce and Ca are both elements that can prevent oxidation and ignition of Mg alloys before casting.[17,18]

For most metals and alloys, their strength can be generally improved by refining grain size.[19] During the solidification processing, there are usually two applicable ways to refine grain size: chemical alloying and physical treatments. Using chemical alloying route to refine microstructures in alloy has long been studied. Although, chemical alloying is an easier way, there is still a long way to go before it could be an effective way to reach the ideal strength that we need.[20,21] In contrast, the physical

treatment method is replied on the stimulation of alloys melts by an external physical field which may introduce intensive shearing effects, for instance, electromagnetic stirring, ultrasonic vibration, pulsed electrical current, etc.[22–24] Rencently, Wannasin[25] et al. creatively invented a method named gas-induced semisolid (GISS) process, which blows Ar gas into the molten Al alloys before solidification to prepare semi-solid slurries contains well-refined nondendritic primary particles in Al alloys. Followed by the work of Wannasin's, Thanabumrungkul[26] et al. proposed the rheo-die casting process and confirmed that fewer porosities were observed in the components of A356 and 7075 Al alloys casting prepared by the rheo-die casting process than conventional die casting process.

To enhance the properties of AZ91 alloy, Zhang[27] in our research group has introduced the GISS method in preparing the semi-solid slurry and rheo-squeeze casting AZ91–Ca alloy. However, the rheo-squeeze casted AZ91–Ca alloy is still lower than the desired strengths [ultimate tensile strength (UTS): 200 MPa; yield strength (YS): 130 MPa]. In addition, the squeeze casting process cannot be used to manufacture complex structure components.

In present work, the alloying element Ce was added into AZ91–2Ca Mg alloy based on Deng's researches to further refine the microstructure and enhance the ignition proof and oxidation behaviors during the melting process.[28] Meanwhile, gas-bubbling process and traditional die casting that has a higher injection speed to reduce the manufacturing time and could get more complex components were used together to rheology form of AZ91–2Ca–1.5Ce alloy, expecting to achieve higher mechanical properties. The semi-solid slurry of the alloy was prepared by Ar gas-bubbling processing and then came to direct die casting and squeeze casting, respectively. The purpose of the experiment was to find the effect of gas-bubbling parameters and pouring temperature on microstructure and tensile strength of rheo-die casting AZ91–2Ca–1.5Ce alloy. Also, the difference between rheo-die casting and rheo-squeeze casting AZ91–2Ca–1.5Ce alloys was studied.

II. EXPERIMENTAL PROCEDURE

A. Materials and sample preparation

The samples used in this work were rheo-die casting and rheo-squeeze casting AZ91–2Ca–1.5Ce (wt%) magnesium alloy. In the present experiments, the commercial AZ91 ingots, pure metal Ca and Mg–90Ce (wt%) master alloy were used to produce AZ91–2Ca–1.5Ce alloys. The actual chemical composition (both rheo-die and rheo-squeeze casting samples) was measured by an inductively coupled plasma analyzer (ICP, Perkin Elmer, Plasma-400) and the result is presented in Table I. First of all, the

AZ91 ingot was melted in a stainless steel crucible, which was protected by an atmosphere of 1% SF_6 and 99% CO_2 (volume fraction) in an electric resistance furnace. Mg–90Ce master alloy was added into the molten alloy at 720 °C and stirred for 4 min, which was done to get a homogeneous distribution of chemical composition. After that, pure metal Ca was added into the melt when the temperature of melt was 680 °C and stirred for 3 min. Before gas bubbling and die/squeeze casting, the melt was kept at 720 °C for 30 min.

The equipment used for blowing Ar gas and rheo-die and rheo-squeeze casting process are visually shown in Fig. 1. The diffuser was made by drilling 1 mm through-holes in the surface of stainless steel pipe. By connecting the pipe to Ar gas bottle, the gas bubbling can be achieved. We can use a thermocouple to monitor the temperature of melt in a metallic cup that can scoop 600 g melt from crucible each time. Once the melt came to 620 °C, it was diffused by the pipe with holes. The gas flow which could be determined with a gas flow meter was varied as 2, 5, and 8 L/min. When the melt came to the stated pouring temperature, 593, 590, and 587 °C, respectively, the stainless steel pipe was extracted and the obtained semi-solid slurry was quickly poured into a pre-heated copper mold to manufacture semi-solid slurry

TABLE I. Chemical composition of AZ91–2Ca–1.5Ce alloy used in this study.

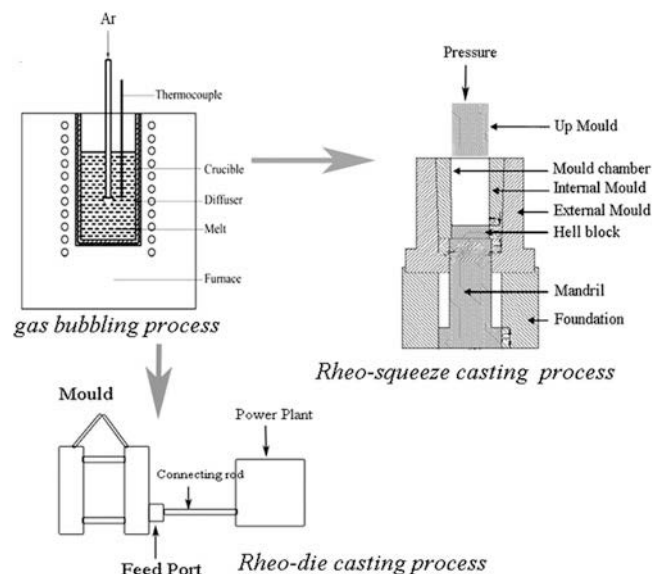| Element	Al	Zn	Ca	Ce	Mg
Objective content (wt%)	9	1	2	1.5	Bal.
Actual content (Rheo-die casting) (wt%)	7.88	0.48	1.76	1.55	Bal.
Actual content (Rheo-squeeze casting) (wt%)	7.70	0.54	1.82	1.46	Bal.

FIG. 1. Illustration of gas-bubbling process, rheo-die, and rheo-squeeze casting process.

samples whose dimension is $\Phi 15$ mm $\times$ 20 mm. In addition, the rest of semi-solid melt was then poured into BD-35OV5 (the die casting machine) to prepare rheo-die casting samples, for which the gauge length was 30 mm and diameter was 5 mm. The mold temperature was 200 °C, and the injection velocity is 2 m/s. In the rheo-squeeze process, the semi-solid melt was quickly casted by direct squeeze casting process. An 80-ton vertical hydraulic pressure was used to touch the semi-solid melt in a preheated 250 °C mold within 5 s and kept for 20 s. The size of samples was $\Phi 55 \times 80$ mm.

B. Microstructural analysis

First of all, an electric-sparking wire-cutting machine was used to cut microstructure specimens from the shaped samples and then processed it with a metallo-graphic phase machine and etched by nitric acid alcohol solution. Then, the metallograph was taken by optical microscope (OM). The quantitative image analysis soft-ware (image-pro plus v6.0) was used to make quantitative metallographic analysis. The shape factor of primary α-Mg particle is calculated as SF $= 4\pi A/p^2$ (A for area of primary particle and P for perimeter).[27]

C. Tensile testing

A Zwick/Roell Z020 tensile machine (Zwick GmbH & Co., Ulm, Germany) was used to test tensile strength with a cross-head speed of 1 mm/min at room temperature. An X-ray diffraction (XRD) using Ni-filtered Cu K_α radiation was used to characterize phase composition. The tensile fracture was observed on a scanning electron microscope (SEM; JEOL-6460, JEOL Ltd., Tokyo, Japan).

III. RESULTS

A. Preparation of semi-solid slurry

Figure 2 shows the microstructures of as-quenched AZ91–2Ca–1.5Ce semi-solid slurry prepared by gas bubbling under different gas-flow rates and cooled to 590 °C. As shown in Fig. 2(a), when the melt is stirred under 2 L/min, the primary α-Mg particles exhibit dendritic morphology in consistent with former report.[27] When increasing the flow rate to 5 L/min, the α-Mg particles have rosette-like shape or roundness and dis-perse more uniformly, and the size of primary particles decreases. As shown in Fig. 2(c), the quantity of the primary α-Mg particle increases, and it produces some inclusions under a flow rate of 8 L/min.

To quantitatively analyze the effect of gas-flow rate on the microstructure of semi-solid slurry, the change rule of average particle size, shape factor, and solid fraction of primary α-Mg particles in AZ91–2Ca–1.5Ce semi-solid slurry prepared could be seen in Fig. 3. It can be seen that the average particle size continuously decreases with the climbing of gas-flow rate. The average grain size of
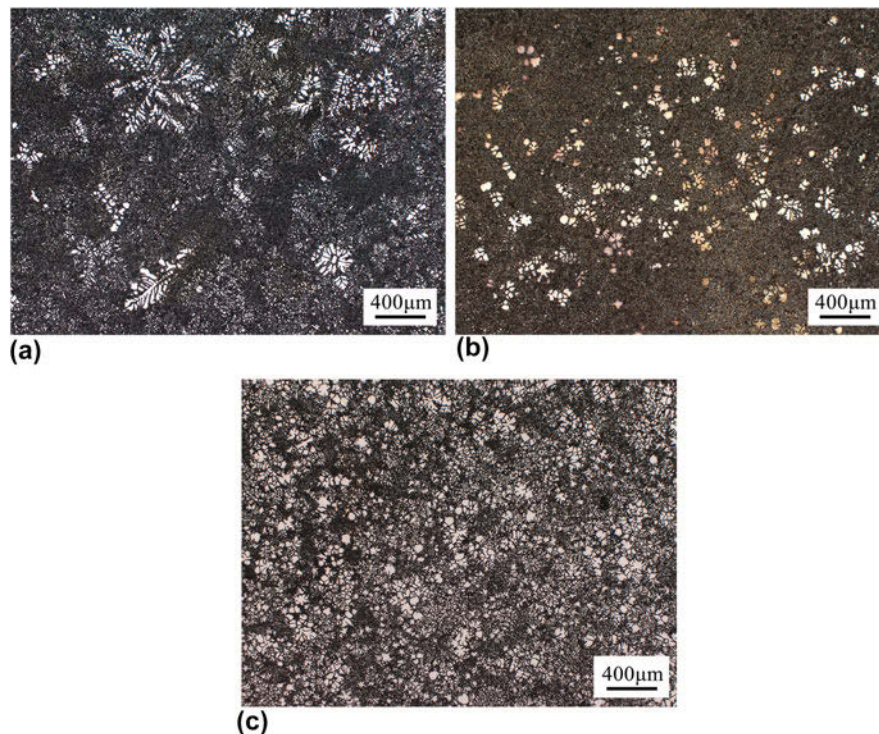

FIG. 2. Optical microstructures of AZ91–2Ca–1.5Ce semi-solid slurry prepared by gas bubbling under different gas-flow rates: (a) 2 L/min; (b) 5 L/min; and (c) 8 L/min.
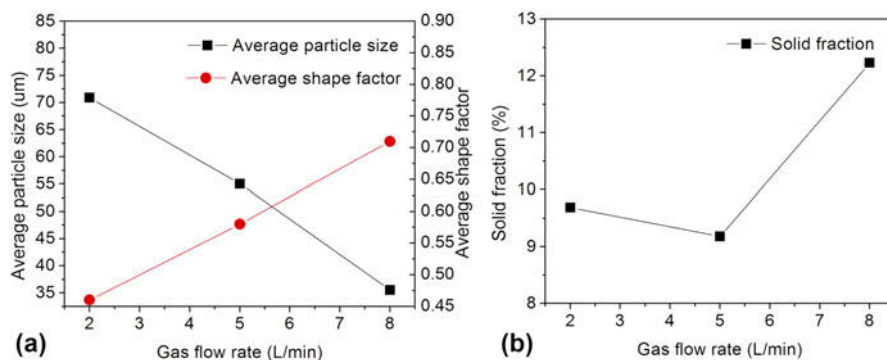
FIG. 3. Effect of gas-flow rate on average size, shape factor, and solid fraction of primary α-Mg particles in AZ91–2Ca–1.5Ce semi-solid slurry: (a) average size and shape factor and (b) solid fraction.

primary phase decreases from 70.88 μm to 55.03 μm when increasing gas the flow rate from 2 L/min to 5 L/min and then decreases to 35.54 μm when gas-flow rate further increases to 8 L/min. On the other hand, the average shape factor of primary α-Mg particles continuously increases along the increasing the gas-flow rate. With the gas-flow rate continuously increasing from 2 L/min to 8 L/min, the average shape factor increases from 0.46 to 0.71. It can also be seen that the solid fraction of primary α-Mg particles changed little under different gas low rate. The former research indicated that further refinement would be negligible although the primary α-Mg particles become more spherical when the gas-flow rate exceeded 5 L/min.[27] Meanwhile, when the gas-flow rate comes to 8 L/min, the melt would drastically splash out, which is very dangerous. When the gas-flow rate is 5 L/min, the appropriate primary particle grain size and shape factor would be obtained which are both beneficial to the final mechanical properties of alloys. So, the gas-flow rate of 5 L/min is chosen for further experiments in our research.

B. Microstructure

Figure 4 shows the microstructures and quantitative analysis of rheo-die casting AZ91–2Ca–1.5Ce alloy samples prepared under different pouring temperatures. It can be easily found that an obviously semi-solid characteristic could be observed by the rheo-die casting process. With the decrease of pouring temperature, the character of primary α-Mg (α1) phase changes obviously, and the size of primary phase continuously increases. As can be seen in Figs. 4(c), α2 phase is the α-Mg phase which formed during the secondary solidification process, the grain size of α2 phase is smaller than α1 phase. Under all experiment pouring temperature, the primary phases distribute homogeneously. When the alloy was poured at 593 °C, the shape of primary particles is round and size is the smallest, comparing to lower pouring temperature. Primary particles mostly developed into rosette-like shape and the solid fraction increased drastically when the pouring temperature was decreased. Meanwhile, the dendritic growth is suppressed to a great extent in samples during rheo-die casting process. When the temperature decreased to 587 °C, the proportion of primary α-Mg phase exceeds 50% which would be obviously harmful to material strength.

Figure 5 shows the OM images and quantitative analysis of the rheo-squeeze casting alloy samples prepared under different pouring temperatures. When the pouring temperature decreases from 593 °C to 587 °C, the microstructure has compelling changes. The grain size and amount of primary α-Mg (α1) phase continuously increase as with rheo-die casting ones, which could be seen in Fig. 5(e). Meanwhile, the second phase begins to concentrate and grows up. As shown in Fig. 5(a), some dendrites which are harmful to mechanical properties of final product can be found. At pouring temperature of 600 °C, the characteristic of α-Mg phase is heterogeneous. Also, some needle-like phase across primary α-Mg phase can be seen under lower pouring temperature. With comparison to the microstructure of rheo-die casting alloy, the microstructure of rheo-squeeze casting alloy does not have obviously semi-solid characteristic.

The XRD patterns of rheo-die and rheo-squeeze casting AZ91–2Ca–1.5Ce alloy under different pouring temperature are presented in Fig. 6. Traditional AZ91 magnesium alloy mainly consists of α-Mg phase and β-$Mg_{17}Al_{12}$ phase.[29] With the addition of Ca and Ce, the content of β-$Mg_{17}Al_{12}$ phase decreases. Meanwhile, two new phases, i.e., Al_2Ca phase and Al_4Ce phase, were generated. It has been reported that a reaction of Al and Ce produced the Al_4Ce phase in the samples of AZ91–Ce magnesium alloy by Cai.[33] For rheo-die casting one as shown in Fig. 6(a), the different pouring temperatures have little effect on the kind and content of different phases expect α-Mg phase, since the intensity and position of diffraction peaks of β-$Mg_{17}Al_{12}$, Al_4Ce, and Al_2Ca under different pouring temperatures have no obviously difference. The intensity of diffraction peak
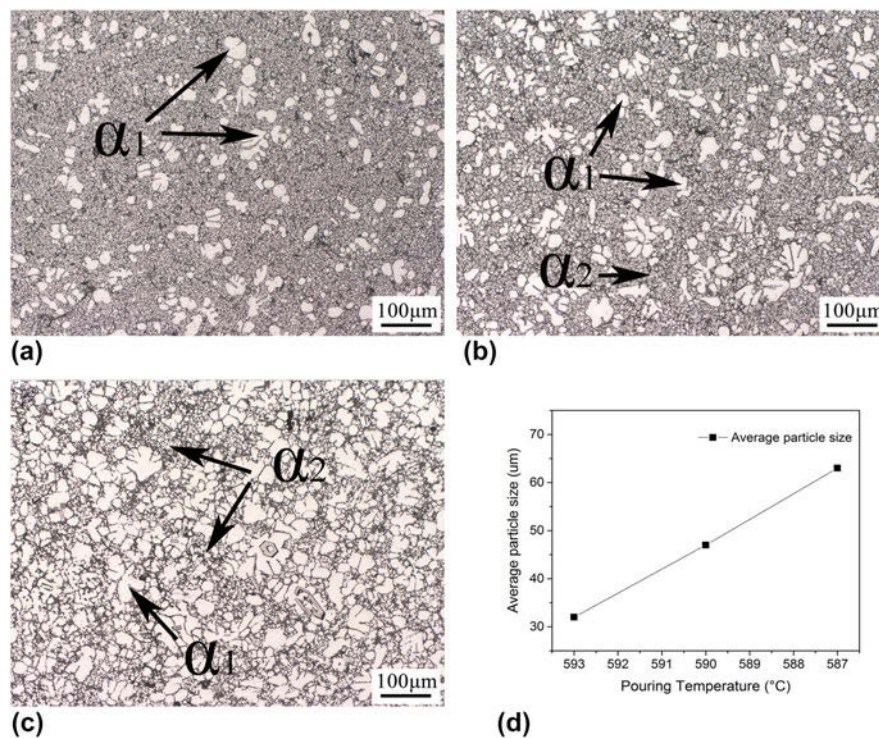
FIG. 4. OM images and quantitative analysis of microstructures of rheo-die casting AZ91–2Ca–1.5Ce alloy samples under different pouring temperatures: (a) 593 °C; (b) 590 °C; (c) 587 °C; and (d) quantitative analysis.

of α-Mg continuously increases when the pouring temperature decreases, which is consistent with the result got from OM images. Figure 6(b) shows the XRD result of rheo-squeeze casting AZ91–2Ca–1.5Ce alloy under different pouring temperatures. For β-$Mg_{17}Al_{12}$, Al_4Ce, and Al_2Ca, it gets similar results with rheo-die casting alloy. As a whole, the α-Mg phase also has no obviously change.

Figure 7(a) and Table II show the SEM analysis results of rheo-die casting AZ91–2Ca–1.5Ce alloy. It is obviously that Ce does not exist in the Mg phase, such as position C in Fig. 7(a). Meanwhile, Ce partly combined with Al to form Al_4Ce phase and remaining distributed at grain boundaries after solidification, as shown in position D in Fig. 7(a). Fig. 7(b) and Table III show the SEM analysis results of rheo-squeeze casting AZ91–2Ca–1.5Ce alloy. We can find in the SEM image that the big block is $Mg_{17}Al_{12}$. The Al_4Ce is the bright needle-like phase, as the C position in Fig. 7(b).

C. Mechanical properties and fracture analysis

The effect of pouring temperature on mechanical properties of rheo-die and traditional die casting (680 °C) AZ91–2Ca–1.5Ce alloy is presented in Fig. 8. It is found that the UTS increases from 186.5 to 202 MPa when the pouring temperature changed from 587 to 590 °C, and then decreases to 188 MPa when the pouring

temperature further increased to 593 °C. Meanwhile, the YS and elongation (EL) appear to have the same tendency as the UTS. It can be found that the peak mechanical properties of the AZ91–2Ca–1.5Ce alloy are significantly higher than those of the die casting AZ91–2Ca–1.5Ce alloy. Compared to die casting alloy, the peaks UTS and EL of rheo-die casting alloy increase by 8 and 64%, while the YS is almost the same. The reason is that rheology process could produce primary α-Mg phase that is a benefit to properties.

Figure 9 shows the mechanical properties of rheo-squeeze casting AZ91–2Ca–1.5Ce alloy under different pouring temperatures. The numbers of tensile strength for rheo-squeeze casting AZ91–2Ca–1.5Ce alloy under different pouring temperatures are indicated in Fig. 9. When the pouring temperature continuously increases from 587 °C to 593 °C, the YS, UTS, and EL also increase. The peak mechanical properties of rheo-squeeze casting AZ91–2Ca–1.5Ce alloy are 98.5 MPa, 170.9 MPa and 3.6%, respectively. When the rheo-squeeze casting AZ91–2Ca–1.5Ce alloy is sent to squeeze machine at 600 °C, the mechanical property slightly decreases, which is consistent with microstructure characteristic. When comparing rheo-die casting alloy to rheo-squeeze one, the peak strength of YS and UTS of rheo-die casting alloy increases by 18 and 56%, respectively. However, the EL decreases by 36%.

Figure 10 shows the fracture surface of tensile tested samples of rheo-die casting AZ91–2Ca–1.5Ce alloy
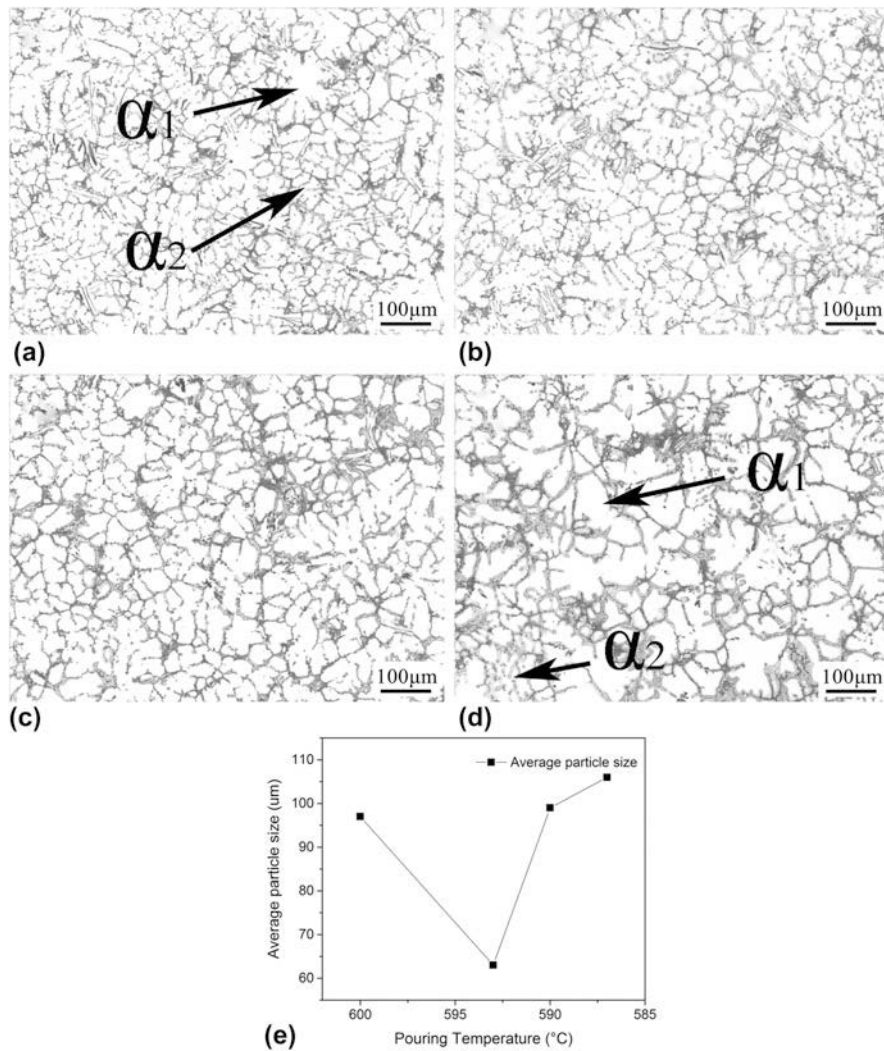
FIG. 5. OM images of microstructures of rheo-squeeze casting AZ91–2Ca–1.5Ce alloy samples under different pouring temperature: (a) 600 °C; (b) 593 °C; (c) 590 °C; (d) 587 °C; and (e) quantitative analysis.
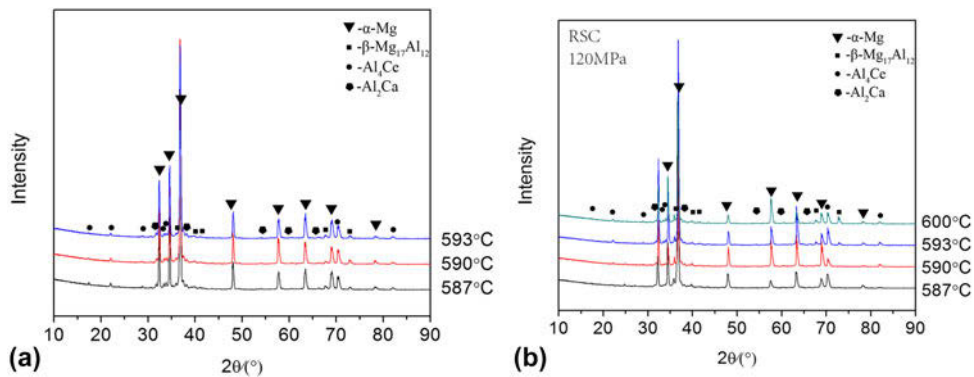

FIG. 6. XRD patterns of different casting AZ91–2Ca–1.5Ce alloy samples under different pouring temperature: (a) rheo-die casing and (b) rheo-squeeze casting.

under different pouring temperatures observed by SEM. As shown in Fig. 10(a), some large ravines and grain boundaries can be observed. In addition, there are a few tearing edges. With comparison to Fig. 10(a), more

tearing edges and cleavage planes could be found in Fig. 10(b), and the fracture surface became more flat. When the pouring temperature decreased to 587 °C, the grain size sharply increased, which was in accordance
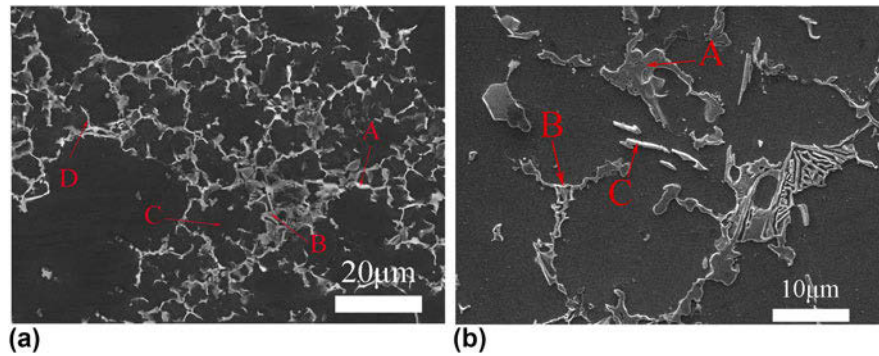
FIG. 7. SEM image of microstructure of different casting AZ91–2Ca–1.5Ce alloy: (a) rheo-die casing and (b) rheo-squeeze casting.

TABLE II. Composition analysis of rheo-die casting AZ91–2Ca–1.5Ce alloy by SEM spot scan.

Site	Mg (wt%)	Al (wt%)	Ca (wt%)	Ce (wt%)
A	79.74	6.22	2.34	1.85
B	61.55	23.69	6.13	0.45
C	86.67	3.47	0.41	0
D	80.39	2.48	1.14	0.33

TABLE III. Composition analysis of rheo-squeeze casting AZ91–2Ca–1.5Ce alloy by SEM spot scan.

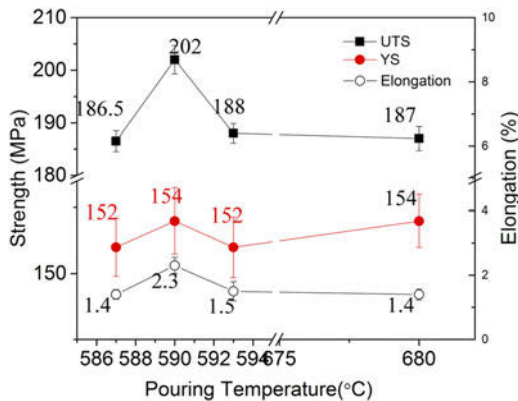| Site	Mg (wt%)	Al (wt%)	Ca (wt%)	Ce (wt%)
A	58.20	41.80	0	0
B	30.60	47.28	22.12	0
C	8.50	37.70	0	53.80

FIG. 8. Effect of pouring temperature on mechanical properties of rheo-die casting AZ91–2Ca–1.5Ce alloy and die casting alloy.
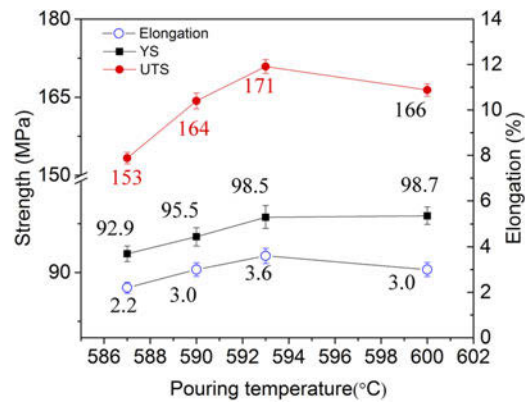

FIG. 9. Effect of pouring temperature on mechanical properties of rheo-squeeze casting AZ91–2Ca–1.5Ce alloy.

Fig. 11. When the pouring temperature is 593 °C, the fracture surface is drastically flat and some stream flows can be seen, as shown in Fig. 11(b). When the temperature changes from 593 °C to 587 °C, more obviously cracks exist in images, as can be seen in Fig. 11(d) where long cracks can be seen and the surface is roughest compare to other state's samples. When the sample was casting at 600 °C, some tearing edges and long crack can be seen in Figs. 11(a) and 11(b).

IV. DISCUSSION

Usually, the AZ91 alloy was consisted of the large dendrite-like α–Mg matrix and the strengthening β–$Mg_{17}Al_{12}$ phase.[29] However, the alloying element Ca could considerably change the morphology of dendrite and precipitate, which decreased the average grain size and refine the second phase originally at grain boundaries. In addition, the bulky strengthening β-$Mg_{17}Al_{12}$ phase was replaced by a framework which formed with skeleton β-$Mg_{17}Al_{12}$ phase and Al_2Ca particles existed within it due to the addition of Ca.[30] The Al_2Ca phase will precipitate firstly, since the higher melting point of Al_2Ca (1352 K).[31,32] In this study, it is observed that AZ91–Ca–Ce alloy prepared by rheo-die

with the OM images. Meanwhile, some large cracks existed in the boundary of the primary α-Mg phase when the melt was poured at 587 °C. These all induced the deterioration of tensile properties.

The fracture surface of tensile tested samples of rheo-squeeze casting AZ91–2Ca–1.5Ce alloy under different pouring temperatures observed by SEM is showed in
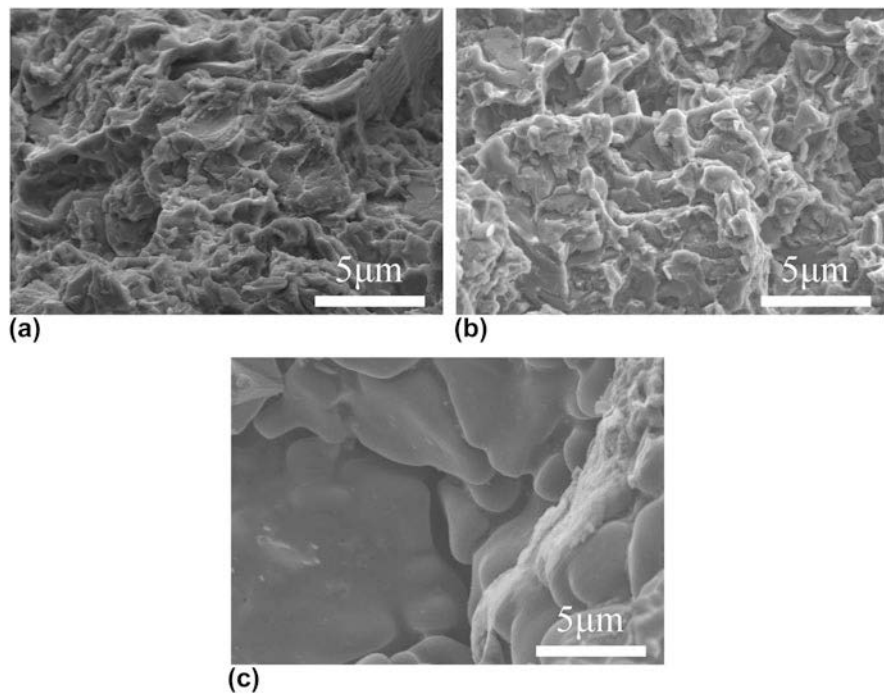
FIG. 10. Fracture surface of tensile tested samples of rheo-die casting AZ91–2Ca–1.5Ce alloy under different pouring temperatures observed by SEM: (a) 593 °C; (b) 590 °C; and (c) 587 °C.
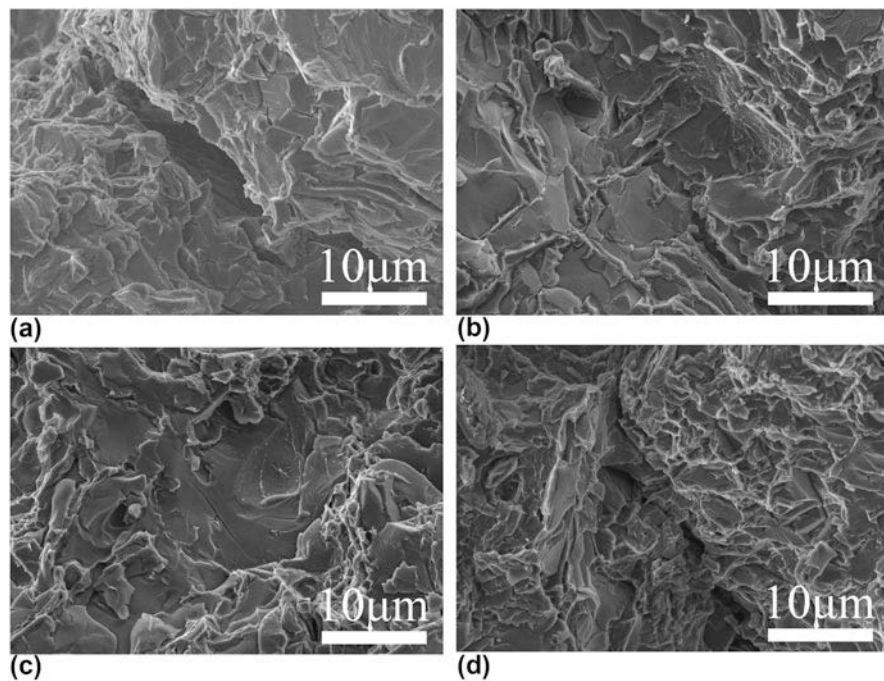

FIG. 11. Fracture surface of tensile tested samples of rheo-squeeze casting AZ91–2Ca–1.5Ce alloy under different pouring temperatures observed by SEM: (a) 600 °C; (b) 593 °C; (c) 590 °C; and (d) 587 °C.

casting exhibit higher tensile strength than existed casting results with the addition of Ca and Ce elements, as shown in Fig. 8. Liu et al.[34] found that the combination addition of Ca and Ce has a better refining effect on the AZ91 alloy. According to Hall–Petch relationship,

$\sigma = \sigma_0 + kd^{-1/2}$, finer grain size primarily results in excellent mechanical properties.

It is found that when increasing the pouring temperature to slightly above the liquid promotes further refinement in microstructure and improvement in

mechanical properties of AZ91–2Ca–1.5Ce alloy on the basis of Ca–Ce addition, as shown in Figs. 4 and 8. It is generally accepted that the pouring temperature would influence the microstructure of as-cast alloy. Xia et al.[35] reported that a pouring temperature just above the liquidus could promote the formation of near-equiaxed primary grains. A pouring temperature as low as 590 °C was chosen because the liquidus temperature of AZ91–Ca alloy is just about 587 °C. Low pouring temperature and fast heat transfer also increase the survival rate of formed nuclei after recalescence. The high level amounts of nuclei limited the growth of particles. Then, concentration gradient before solid–liquid interface decreases and therefore suppresses the dendritic growth. In this study, when the melt of AZ91–2Ca–1.5Ce alloy was poured into the die-casting machine below 600 °C, a large amount of α-Mg nuclei formed in the melt. Due to the high density of nuclei, the growth front of adjacent particles contacted quickly and the growth was then stopped, which led to the formation of rosette-like grains rather than well-developed dendritic. When the temperature decreased from 593 °C to 590 °C, the microstructure was further refined and the amount of primary α-Mg phase increased appropriately, which led to higher mechanical properties, as shown in Figs. 4 and 8. When the pouring temperature further decreased to 587 °C, the grain size of α-Mg increased and the amount of α-Mg increased to a detrimental quantity. It can also be observed that the mechanical properties of AZ91–2Ca–1.5Ce alloy decreased when the pouring temperature decreased from 590 °C to 587 °C.

Comparing Figs. 8 and 9, it can be found that the peak mechanical properties of rheo-die casting AZ91–2Ca–1.5Ce alloys are drastically higher than rheo-squeeze casting AZ91–2Ca–1.5Ce alloys. Despite the elongation of rheo-die casting alloy is a bit lower than that of rheo-squeeze casting alloy. As shown in Fig. 5(b), the amount of primary α-Mg phase in rheo-squeeze casting sample exceeds 50%, which is damaged to tensile strength. However, the amount of α-Mg phase in rheo-die casting sample is around 30%, as can be seen in Fig. 4(b). Meanwhile, the second phases evenly distribute in matrix of rheo-die casting alloy, which can be found in Fig. 4(b). Compared with that, the second phases do not evenly distribute, and some needle-like second phases also exist around matrix which would deteriorate properties of alloy, as shown in Fig. 5(b). The core which made the difference between rheo-die and rheo-squeeze alloys is the difference of casting methods. Under die casting process, the semi-solid slurry was rapidly processed to cast, the fewer process time would better reserve the semi-solid characteristic of slurry. By contrast, the male mold of squeeze machine slowly moved before and during the squeeze process, which would usually miss the optimal opportunity of semi-solid forming process.

V. CONCLUSIONS

In present work, semi-solid slurry of AZ91–2Ca–1.5Ce alloy was prepared by gas bubbling and then casting alloy was formed by die casting and squeeze casting process. The effect of processing parameters on microstructure and mechanical properties of rheo-die casting and rheo-squeeze casting AZ91–2Ca–1.5Ce alloy were studied. The fine semi-solid slurry could be obtained under the gas-flow rate of 5 L/min. For the strength of alloys under different processes, the rheo-die casting AZ91–2Ca–1.5Ce alloy has higher strength than both traditional die casting and rheo-squeeze casting alloy. The detailed conclusions are listed as follows:

(1) The semi-solid slurry of targeted alloy was successfully fabricated by the GISS process. With increasing gas-flow rate from 2 L/min to 5 L/min and keeping the pouring temperature of 590 °C, the primary α-Mg particles change from dendrite to rosette-like shape or roundness and the grain size decreases. With further increasing gas-flow rate to 8 L/min, the microstructure of semi-solid slurry contains inclusions. The best semi-solid slurry could be obtained when the gas-flow rate is 5 L/min, and the average grain size, shape factor, and solid fraction are 55.03 μm, 0.58 and 9.18%.

(2) For the rheo-die casting alloy, when the pouring temperature increases from 587 °C to 593 °C, the grain size of primary α-Mg particles in microstructure continuously decreases. Since the role of primary α-Mg particle introduced by gas-bubbling process, the tensile strength of rheo-die casting AZ91–2Ca–1.5Ce alloy is higher than that of traditional die casting method (UTS = 187 MPa, YS = 154 MPa, and elongation = 1.4%). The peak UTS, YS, and elongation of rheo-die casting alloy are 202 MPa, 154 MPa, and 2.3% when the pouring temperature is 590 °C.

(3) When the pouring temperature of rheo-squeeze casting alloys increases from 587 °C to 593 °C, the grain size of primary α-Mg particles decreases. However, with further increasing pouring temperature to 600 °C, the grain size begins to increase. Accordingly, the mechanical properties increases firstly and then decreases with continuously increasing pouring temperature. When the pouring temperature of rheo-squeeze casting alloy is 593 °C, the peak UTS, YS, and elongation are 171 MPa, 98.5 MPa, and 3.6%, respectively.

(4) For the two rheology casting processes, the peak strength of rheo-die casting AZ91–2Ca–1.5Ce alloys are drastically higher than rheo-squeeze casting AZ91–2Ca–1.5Ce alloys. The main reason that made the difference between rheo-die and rheo-squeeze alloys is the characteristic of primary α-Mg particles and distribution of secondary phase, which is caused by casting process. Under die casting process, the semi-solid slurry was rapidly processed to cast, the fewer process time would

better reserve the semi-solid characteristic of slurry. By contrast, the male mold of squeeze machine slowly moved before and during the squeeze process, which would usually miss the optimal opportunity of semi-solid forming process.

ACKNOWLEDGMENTS

REFERENCES

1. H. Zhang, H.J. Li, Q.Y. Guo, Y.C. Liu, and L.M. Yu: Hot deformation behavior of Ti–22Al–25Nb alloy by processing maps and kinetic analysis. *J. Mater. Res.* **31**(12), 1764 (2016).

2. W.C. Liu, L.K. Jiang, L. Cao, J. Mei, G.H. Wu, S. Zhang, L. Xiao, S.H. Wang, and W.J. Ding: Fatigue behavior and plane-strain fracture toughness of sand-cast Mg–10Gd–3Y–0.5Zr magnesium alloy. *Mater. Des.* **59**, 466 (2014).

3. M.G. Jiang, H. Yan, L. Gao, and R.S. Chen: Microstructural evolution of Mg–7Al–2Sn Mg alloy during multi-directional impact forging. *J. Magnesium Alloys* **3**, 180 (2015).

4. Y.L. Li, G.H. Wu, A.T. Chen, and H.R. Jafari Nodooshan: Effect of Gd and Zr additions on the microstructure and high-temperature mechanical behavior of Mg–Gd–Y–Zr magnesium alloys in the product form of a large structural casting. *J. Mater. Res.* **30**, 3461 (2015).

5. J.H. Zhang, X.D. Niu, X. Qiu, K. Liu, and C.M. Nan: Effect of yttrium-rich misch metal on the microstructures, mechanical properties and corrosion behavior of die cast AZ91 alloy. *J. Alloys Compd.* **471**, 322 (2009).

6. P. Bakke and H. Westengen: Die casting for high performance—Focus on alloy development. *Adv. Eng. Mater.* **5**(12), 879 (2003).

7. L.L. Guo and F. Fujita: Influence of rolling parameters on dynamically recrystallized microstructures in AZ31 magnesium alloy sheets. *J. Magnesium Alloys* **3**, 95 (2015).

8. A. Luo: Recent magnesium alloy development for elevated temperature applications. *Int. Mater. Rev.* **49**, 13 (2004).

9. G. Pettersen, H. Westengen, R. Hoier, and O. Lohne: Microstructure of a pressure die cast magnesium—4 wt% aluminium alloy modified with rare earth additions. *Mater. Sci. Eng., A* **207**(1), 115 (1996).

10. L. Shepeleva and M. Bamberger: Microstructure of high pressure die cast AZ91D modified with Ca and Ce. *Mater. Sci. Eng., A* **425**(1–2), 312 (2006).

11. G.L. Song, A.L. Bowles, and D.H. StJohn: Corrosion resistance of aged die cast magnesium alloy AZ91D. *Mater. Sci. Eng., A* **366**(1), 74 (2004).

12. Y.P. Wu, X.M. Zhang, Y.L. Deng, and C.P. Tang: Microstructure, texture, and enhanced mechanical properties of an extruded Mg-rare earth alloy after hot compression. *J. Mater. Res.* **30**(24), 3776 (2015).

13. F. Xue, X.G. Min, and Y.S. Sun: Microstructures and mechanical properties of AZ91 alloy with combined additions of Ca and Si. *J. Mater. Sci.* **41**, 4725 (2006).

14. H.L. Zhao, S.K. Guan, and F.Y. Zheng: Effects of Sr and B addition on microstructure and mechanical properties of AZ91 magnesium alloy. *J. Mater. Res.* **22**(9), 2423 (2007).

15. J.C. Yu, Z. Liu, Y. Dong, and Z. Wang: Dynamic compressive property and failure behavior of extruded Mg–Gd–Y alloy under high temperatures and high strain rates. *J. Magnesium Alloys* **3**, 134 (2015).

16. J.L. Wang, R.L. Liao, L.D. Wang, Y.M. Wu, Z.Y. Cao, and L.M. Wang: Investigations of the properties of Mg–5Al–0.3Mn–xCe (x = 0–3, wt%) alloys. *J. Alloys Compd.* **477**(1–2), 341 (2009).

17. J.G. Chen, Y. Sun, J.S. Zhang, W.L. Cheng, X.F. Niu, and C.X. Xu: Effects of Ti addition on the microstructure and mechanical properties of Mg–Zn–Zr–Ca alloys. *J. Magnesium Alloys* **3**, 121 (2015).

18. M. Sakamoto and S. Akiyama: Suppression of ignition and burning of molten Mg alloys by Ca bearing stable oxide film. *J. Mater. Sci. Lett.* **16**, 1048 (1997).

19. D.H. StJohn, M. Qian, M.A. Easton, P. Cao, and Z. Hildebrand: Grain refinement of magnesium alloys. *Metall. Mater. Trans. A* **36**, 1669 (2005).

20. Y. Turen: Effect of Sn addition on microstructure, mechanical and casting properties of AZ91 alloy. *Mater. Des.* **49**, 1009 (2013).

21. R. Shabadi, R. Ambat, and E.S. Dwarakadasa: AZ91C magnesium alloy modified by Cd. *Mater. Des.* **53**, 445 (2014).

22. C. Limmaneevichitr, S. Pongananpanya, and J. Kajornchaiyakul: Metallurgical structure of A356 aluminum alloy solidified under mechanical vibration: An investigation of alternative semi-solid casting routes. *Mater. Des.* **30**, 3925 (2009).

23. F. Taghavi, H. Saghafian, and Y.H.K. Kharrazi: Study on the ability of mechanical vibration for the production of thixotropic microstructure in A356 aluminum alloy. *Mater. Des.* **30**, 115 (2009).

24. C.L. Wang, A.T. Chen, L. Zhang, W.C. Liu, G.H. Wu, and W.J. Ding: Preparation of an Mg–Gd–Zn alloy semisolid slurry by low frequency electro-magnetic stirring. *Mater. Des.* **84**, 53 (2015).

25. J. Wannasin, R. Martinez, and M. Flemings: Grain refinement of an aluminum alloy by introducing gas bubbles during solidification. *Scr. Mater.* **55**, 115 (2006).

26. S. Thanabumrungkul, S. Janudom, R. Burapa, P. Dulyapraphant, and J. Wannasin: Industrial development of gas induced semi-solid process. *Trans. Nonferrous Met. Soc. China* **20**, 1016 (2010).

27. Y. Zhang, G.H. Wu, W.C. Liu, L. Zhang, S. Pang, and W.J. Ding: Effects of processing parameters on microstructure of semi-solid slurry of AZ91D magnesium alloy prepared by gas bubbling. *Trans. Nonferrous Met. Soc. China* **25**, 2181 (2015).

28. Z.H. Deng, H.J. Li, W.J. Zhao, and W.B. Li: Effects of Ce concentrations on ignition temperature and surface tension of Mg–9 wt% Al alloy. *China Foundry* **10**(2), 108 (2013).

29. G.Y. Yuan, Y.S. Sun, and W.J. Ding: Effects of Sb addition on the microstructure and mechanical properties of AZ91 magnesium alloy. *Scr. Mater.* **43**, 1009 (2000).

30. L. Lin, F. Wang, L. Yang, L.J. Chen, Z. Liu, and Y.M. Wang: Microstructure investigation and first-principle analysis of die-cast AZ91 alloy with calcium addition. *Mater. Sci. Eng., A* **528**, 5283 (2011).

31. R. Ninomiya, T. Ojiro, and K. Kubota: Improved heat resistance of Mg–Al alloys by the Ca addition. *Acta Metall. Mater.* **43**(2), 669 (1995).

32. T. Miyazaki, J. Kaneko, and M. Sugamata: Structures and properties of rapidly solidified Mg–Ca based alloys. *Mater. Sci. Eng., A* **181–182**, 1410 (1994).

33. H.S. Cai, F.F. Guo, X.S. Ren, J. Su, and B.D. Chen: Effects of cerium on as-cast microstructure of AZ91 magnesium alloy under different solidification rates. *J. Mater. Process. Technol.* **34**(7), 736 (2016).

34. S.F. Liu, B. Li, X.H. Wang, W. Su, and H. Han: Refinement effect of cerium, calcium and strontium in AZ91 magnesium alloy. *J. Mater. Process. Technol.* **209**, 3999 (2009).

35. K. Xia and G. Tausig: Liquidus casting of a wrought aluminum alloy 2618 for thixoforming. *Mater. Sci. Eng., A* **246**(1–2), 1 (1998).